

# Assessment of Average Muscle Fiber Conduction Velocity From Surface EMG Signals During Fatiguing Dynamic Contractions

Dario Farina\*, *Member, IEEE*, Marco Pozzo, Enrico Merlo, Andrea Bottin, and Roberto Merletti, *Member, IEEE*

**Abstract**—In this paper, we propose techniques of surface electromyographic (EMG) signal detection and processing for the assessment of muscle fiber conduction velocity (CV) during dynamic contractions involving fast movements. The main objectives of the study are: 1) to present multielectrode EMG detection systems specifically designed for dynamic conditions (in particular, for CV estimation); 2) to propose a novel multichannel CV estimation method for application to short EMG signal bursts; and 3) to validate on experimental signals different choices of the processing parameters. Linear adhesive arrays of electrodes are presented for multichannel surface EMG detection during movement. A new multichannel CV estimation algorithm is proposed. The algorithm provides maximum likelihood estimation of CV from a set of surface EMG signals with a window limiting the time interval in which the mean square error (mse) between aligned signals is minimized. The minimization of the windowed mse function is performed in the frequency domain, without limitation in time resolution and with an iterative computationally efficient procedure. The method proposed is applied to signals detected from the vastus lateralis and vastus medialis muscles during cycling at 60 cycles/min. Ten subjects were investigated during a 4-min cycling task. The method provided reliable assessment of muscle fatigue for these subjects during dynamic contractions.

**Index Terms**—Conduction velocity estimation, dynamic EMG, linear electrode arrays, surface electromyography.

## I. INTRODUCTION

MUSCLE fiber conduction velocity (CV) is an important physiological parameter which provides information regarding fiber membrane properties, fiber contractile characteristics [1], and peripheral muscle fatigue [2]–[4]. CV may change as a consequence of pathology [5] and is indicative of muscle fiber type constituency and particular muscle training [6].

Estimation of muscle fiber CV can be performed by means of either intramuscular or surface electromyographic (EMG) recordings [2], [7], [8]. Methods based on invasive techniques are time consuming, painful, and inherently limited to

controlled experimental conditions [7]. Surface EMG based techniques for CV estimation are noninvasive and can be applied more easily than intramuscular ones. However, the estimation of muscle fiber CV from surface recordings is troublesome; it indeed requires expert operators for electrode positioning and is affected by many factors other than the physiological phenomena under study [9]. Because of these difficulties, many researchers have applied surface EMG spectral analysis for indirect assessment of muscle fiber CV.

The theoretical derivation by Lindstrom and Magnusson [10] indicates that the relative changes of characteristic spectral frequencies are equal to those of CV [11], [12]. This observation, which is correct within reasonable approximations during constant force, constant posture, isometric contractions [11], has been extended to different conditions, such as variable force isometric (e.g., [13]) or dynamic contractions (e.g., [14]).

The issue of extending muscle fiber CV assessment from constant force, isometric contractions to dynamic tasks poses serious difficulties. On the other hand, dynamic contractions are closer to daily life activities than standardized laboratory conditions. The assessment of muscle fiber membrane properties in these conditions allows better insight into muscle fatigue and coordination, with applications in basic physiology, ergonomics, sport medicine, and occupational medicine, among other fields. However, due to technical limitations, reliable estimation of CV during movement was not possible and spectral estimation has been the method of choice. Along this line, different spectral analysis techniques have been tested and compared on non-stationary surface EMG signals [14]–[17]. However, the relative simplicity of application of surface EMG spectral analysis should be countered by the difficulty in interpreting results on a physiological basis.

We devoted part of our research in the last years to developing and applying methods for multichannel surface EMG signal detection and estimation of muscle fiber CV. We proposed techniques for separating single-motor-unit action potentials (MUAPs) from the interference EMG signal and estimating their CV [18] and for reducing variance [3], [19] and bias [20] of CV estimates. We also analyzed experimentally and by simulations the sources of error of CV estimation [9], [21] and the relationships between CV and spectral EMG features in different conditions, including recruitment/de-recruitment of motor units (MUs) [22]. In this work we propose the application of advanced methods for CV estimation during dynamic contractions. A fatiguing cycling task will be analyzed.

The main objectives of this study are: 1) to present multi-electrode EMG detection systems specifically designed for dy-

Manuscript received April 4, 2003; revised November 1, 2003. This work was supported in part by the European Shared Cost Project Neuromuscular assessment in the Elderly Worker (NEW) (QLRT-2000-00139), by Contract C15097/01/NL/SH of the European Space Agency (ESA) on Microgravity effects on skeletal muscles investigated by surface EMG and mechanomyogram, by the Italian Space Agency (Contract ASI I/R/137/01), and by PRIMA Biomedical and Sport, Treviso, Italy. *Asterisk indicates corresponding author.*

\*D. Farina is with the Center of Bioengineering, Department of Electronics, Politecnico di Torino, Torino 10129, Italy (e-mail: dario.farina@polito.it).

M. Pozzo, E. Merlo, A. Bottin, and R. Merletti are with the Center of Bioengineering, Department of Electronics, Politecnico di Torino, Torino 10129, Italy.

Digital Object Identifier 10.1109/TBME.2004.827556

dynamic conditions (in particular, for CV estimation); 2) to propose a multichannel CV estimation method for application to short EMG bursts of activity; and 3) to validate on experimental signals the methods proposed for different choices of the processing parameters.

## II. METHODS

In the following, we propose a set of procedures for detecting and analysing signals during dynamic conditions by multichannel recordings. Innovative sensors as well as processing techniques will be presented and applied together with methods already described in previous work. Finally, the experimental protocol adopted for validating the techniques is described and results are reported.

### A. Multichannel Surface EMG Detection During Dynamic Contractions

Although CV can be theoretically estimated from the location of the spectral dips of a single differential EMG derivation [10], [23], this estimation method suffers of large estimation variance [24]. With the purpose of reliably estimating muscle fiber CV, surface EMG signals should be detected from at least two locations over the skin. Spatial filtering may be applied to each detection point. A one-dimensional or a two-dimensional electrode array is generally used for assessing CV in isometric, constant force contractions [25]. However, in the case of movement, a dry array of metal electrodes may be critical because of large artifacts generated at the skin-electrode interface. We thus developed adhesive linear arrays of a number of equi-spaced electrodes for which conductive gel assures proper skin-electrode contact. These arrays have been patented (LISiN-SPES Medica, Italian patent number GE2001A000 086) and tested in different conditions [26]. The silver-silver chloride interface is separated from the skin by a small cavity (about 1-mm thick) filled with electrolyte gel (Fig. 1); the fluid gel between the electrode and the skin acts as a buffer in the event of movement [26], [27].

In this study, we used adhesive arrays of eight electrodes, with 5 mm interelectrode distance and 5 mm  $\times$  1 mm electrode cavities, whose size matched the fiber semi-length of the investigated muscles (see Experimental Protocol). 20–30  $\mu$ L of conductive gel for each electrode of the array was used to assure proper electrode-skin contact and was inserted with a gel dispenser (model Eppendorf AG—Multipette plus, Hamburg, Germany) into the cavities of the adhesive electrode array. Fig. 1 shows the location of the adhesive electrode arrays over the vastus lateralis and medialis muscles during an experimental session.

Electrode location is critical for assessing muscle fiber CV, as well as other surface EMG derived variables (e.g., [28], [29]). During movement, the problems related to the variability of EMG variable estimates with electrode location are more serious than in isometric contractions. The muscle fiber length indeed changes during movement and the relative position of the electrodes with respect to the innervation zones and tendons may vary. For reliable estimation of CV during a dynamic task, the electrodes from which EMG signals are detected should be located between the innervation zone and tendon in all the conditions (i.e., at all joint angles). The movement of the electrodes

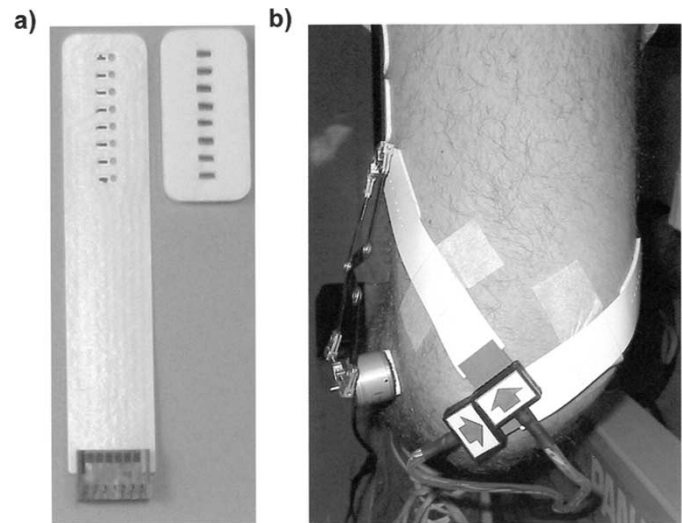


Fig. 1. (a) The linear array used in this study. The disposable part (on the right) is adhesive on the two sides and is attached to the reusable part (on the left). (b) The arrays were located over the vastus lateralis and medialis muscles. A goniometer is also used to record the joint angle. The two arrays are distal with respect to the most distal location of the detected innervation zones. Note the flexibility of the arrays which allow adaptation to the skin curvature (in this case particularly evident for the vastus medialis muscle).

with respect to the muscle fibers is particularly critical for CV estimation when the innervation zone passes under the detection electrodes at certain joint angles [30]. The amount of electrode relative movement depends largely on the muscle [31]. Since the surface arrays should be between the innervation zone and tendon region at all the joint angles of interest, the location of the innervation zone should be identified at the extreme joint angles, in preliminary test contractions (see Experimental Protocol).

### B. Detection of Muscle Activity During a Dynamic Task

In a dynamic task, the muscle may be active only during certain time intervals. The intervals of activity should be estimated from the characteristics of the EMG signals. We recently developed a method for detecting bursts of EMG activity in additive noise [32]. The method is based on a bank of filters whose impulse response is matched to the MUAP shape. The method applied to a single channel provides better performance at a lower computational cost than previously developed techniques [32]. In this work, the method proposed in [32] was applied to all the signals of the array independently; the activation intervals were defined as those common to all the signals, i.e., as the logic AND of the Boolean activation functions of the individual channels.

### C. Windowed Multichannel CV Estimators

Various algorithms to estimate CV exist, at the global and single MU level [2], [3], [18]–[20], [24], [33]–[39]. Two-channel based CV estimates suffer from high variance which can be reduced using multichannel approaches [19], [40]. In this study, we developed and applied a novel multichannel algorithm for low variance estimation of CV. The algorithm is implemented in the frequency domain and, thus, is not limited by the inherent time resolution implied by the sampling process (if the Nyquist criterion is satisfied); it is based on the concepts proposed in [19] with specific features for application to short signal bursts.

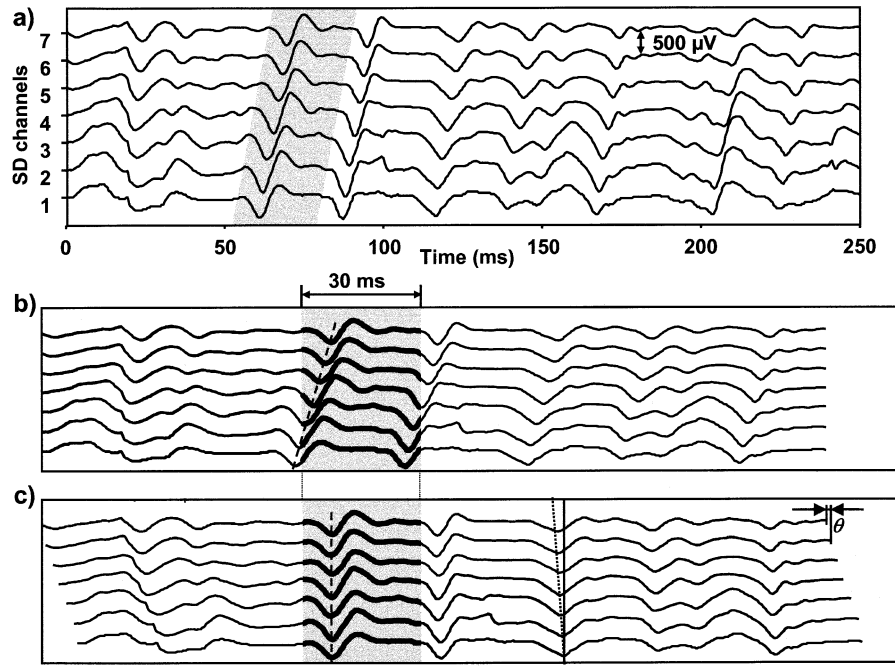


Fig. 2. (a) Surface EMG signals detected from the vastus medialis muscle during a cycling task. Propagating MUAPs are clearly visible. (b) An example of windowing of the multichannel signals. The MUAPs are truncated when travelling along the array and signal alignment within the window is critical. A very short window is applied to outline the truncation effect. (c) Signal alignment followed by windowing of the signals which avoids signal truncation.

Consider a set of signals delayed with respect to each other and added to different independent, white, zero mean, Gaussian noises  $w_k(t)$  with equal variance  $\sigma^2$

$$\begin{aligned} x_k(t) &= s(t - (k-1)\theta) + w_k(t) \\ k &= 1, \dots, K; \quad 0 \leq t \leq T \end{aligned} \quad (1)$$

where  $\theta$  is the delay between adjacent channels and  $T$  the duration of the observed signal. The model described by (1) is valid only for a set of signals  $x_k(t)$  with limited temporal support, shorter than  $T$  (in case  $\theta \neq 0$ ). If the latter condition is not valid, a truncation occurs and (1) is not exact (Fig. 2). This effect is negligible when  $T$  is large but may be relevant when short signal portions are considered (e.g., epochs of the duration of a few MUAPs). In the case of a burst of activity detected by different channels, (1) can be exactly applied since the signal is temporally limited. Similar considerations hold for single MU CV estimation when MUAPs are extracted and isolated from the interference EMG signal [3], [19]. However, to analyze different phases of activity in dynamic conditions, each burst should be divided into segments. Considering that bursts of EMG activity may have a duration of hundreds of milliseconds, portions of these bursts have a duration of tens of milliseconds, comparable to MUAP duration.

In the case of two channels, to estimate CV avoiding MUAP truncation, one channel could be shifted with respect to the other by a delay  $\theta$  by multiplying its Fourier transform by  $e^{-j2\pi f\theta}$  and transforming back in the time domain. The mean square error (mse) between the two channels could then be computed in the time domain only within the window of interest and minimized by exhaustive search of the optimal value of  $\theta$ . Similar considerations hold for the multichannel case. In previous work, we applied this approach for single MUAP multichannel CV estimation when the MUAPs could not be completely isolated from each other [18]. This approach is computationally demanding

since it does not apply an iterative technique for optimal delay estimation but rather makes use of an exhaustive search. Exhaustive search also implies that the time resolution is limited by the selected step with which the signals are shifted. In the following, we will describe a multichannel maximum likelihood estimation method in the frequency domain which allows estimation of CV by windowing the signal in time domain but without any signal truncation.

From (1), the maximum likelihood criterion for delay estimation leads, in the discrete case, to minimization of the following mse [19], function of  $\theta$

$$e_{MLE}^2 = \left(1 - \frac{1}{K}\right) \sum_{k=1}^K e_k^2 \quad (2)$$

where  $K$  is the number of channels,  $N$  the number of samples in the entire signal support time  $[T$  in (1)], and

$$e_k^2 = \sum_{n=1}^N \left( x_k(n) - \frac{1}{K-1} \sum_{m=1, m \neq k}^K x_m(n + (m-k)\theta) \right)^2 \quad (3)$$

The mse function in (2) is the mean of the  $K$  errors between channel  $k$  and the average of the other  $(K-1)$  channels, after application of a temporal shift multiple of  $\theta$  (for signal alignment).

To estimate CV in a certain subwindow of the time interval  $T$ , the mses in (3) become

$$\begin{aligned} \hat{e}_k^2 &= \sum_{n=1}^N \left[ p(n) \cdot \left( x_k(n) - \frac{1}{K-1} \right. \right. \\ &\quad \cdot \left. \left. \sum_{m=1, m \neq k}^K x_m(n + (m-k)\theta) \right)^2 \right] \end{aligned} \quad (4)$$

where  $p(n)$  is the window selected. Note that, if  $\theta \neq 0$ , (4) is not equivalent to the segmentation of the multichannel signal in (1)

by the window  $p(n)$  followed by the computation of the mse between the windowed signal  $x_k(n)$  and the other aligned signals. In that case, indeed, truncation occurs. There is no truncation in (4), since first the signals are shifted and then the window is applied to limit the computation of the mse to the time interval of interest (Fig. 2). The window  $p(n)$  implied in (4) can be of any shape, not necessarily rectangular.

Equation (4) can be written as

$$\begin{aligned} \hat{e}_k^2 &= \sum_{n=1}^N \left( \sqrt{p(n)} \cdot x_k(n) - \frac{1}{K-1} \sqrt{p(n)} \right. \\ &\quad \cdot \left. \sum_{m=1, m \neq k}^K x_m(n + (m-k)\theta) \right)^2 \\ &= \sum_{n=1}^N \left( q(n) \cdot x_k(n) - \frac{1}{K-1} \right. \\ &\quad \cdot \left. \sum_{m=1, m \neq k}^K (q(n) \cdot x_m(n + (m-k)\theta)) \right)^2 \quad (5) \end{aligned}$$

with  $q(n) = \sqrt{p(n)}$  being the square root of the window applied to the mse. Equation (5) can be applied in an exhaustive way by shifting the signals in the frequency domain and computing the mse in the temporal domain with the application of the selected window. A better approach is to directly compute the mse in the frequency domain. Equation (5) becomes, in the frequency domain

$$\begin{aligned} \hat{e}_k^2 &= \frac{2}{N} \sum_{\alpha=1}^{N/2} \left| Q(\alpha) * X_k(\alpha) - \frac{1}{K-1} \right. \\ &\quad \cdot \left. \sum_{m=1, m \neq k}^K [Q(\alpha) (X_m(\alpha) e^{j2\pi\alpha(m-k)\theta/N})] \right|^2 \\ &= \frac{2}{N} \sum_{\alpha=1}^{N/2} |\gamma(\alpha, \theta)|^2 \quad (6) \end{aligned}$$

where  $*$  indicates the convolutive product,  $\alpha$  is the discrete frequency,  $Q(\alpha)$  is the Fourier transform of  $q(n)$ , and  $X_i(\alpha)$  is the Fourier transform of the signals  $x_i(n)$ .

From the first and second derivative of  $\hat{e}_k^2$ , the Newton method can be applied for the minimization of the mse function. This avoids exhaustive search of the minimum, saving computational time. We obtain, with the notation of (6)

$$\begin{aligned} \frac{d\hat{e}_k^2}{d\theta} &= \frac{4}{N} \sum_{\alpha=1}^{N/2} \left[ \text{Re}\{\gamma(\alpha, \theta)\} \frac{d\text{Re}\{\gamma(\alpha, \theta)\}}{d\theta} \right. \\ &\quad \left. + \text{Im}\{\gamma(\alpha, \theta)\} \frac{d\text{Im}\{\gamma(\alpha, \theta)\}}{d\theta} \right] \\ \frac{d^2\hat{e}_k^2}{d\theta^2} &= \frac{4}{N} \sum_{\alpha=1}^{N/2} \left\{ \left[ \frac{d\text{Re}\{\gamma(\alpha, \theta)\}}{d\theta} \right]^2 \right. \\ &\quad + \text{Re}\{\gamma(\alpha, \theta)\} \frac{d^2\text{Re}\{\gamma(\alpha, \theta)\}}{d\theta^2} \\ &\quad + \left[ \frac{d\text{Im}\{\gamma(\alpha, \theta)\}}{d\theta} \right]^2 \\ &\quad \left. + \text{Im}\{\gamma(\alpha, \theta)\} \frac{d^2\text{Im}\{\gamma(\alpha, \theta)\}}{d\theta^2} \right\} \quad (7) \end{aligned}$$

where  $\text{Re}\{\cdot\}$  and  $\text{Im}\{\cdot\}$  stand for real and imaginary part, respectively. The terms in (7) are obtained as follows:

$$\begin{aligned} \text{Re}\{\gamma(\alpha, \theta)\} &= \frac{1}{K-1} \\ &\quad \cdot \sum_{m=1, m \neq k}^K \left[ \text{Re}\{X_k(\alpha) * Q(\alpha)\} \right. \\ &\quad \left. - \text{Re}\left\{ \left( X_k(\alpha) e^{j2\pi\alpha(m-k)\theta/N} \right) * Q(\alpha) \right\} \right] \\ \frac{d\text{Re}\{\gamma(\alpha, \theta)\}}{d\theta} &= \frac{1}{K-1} \\ &\quad \cdot \sum_{m=1, m \neq k}^K \left[ \text{Im}\left\{ \left( X_k(\alpha) \frac{2\pi\alpha(m-k)}{N} \right) \right. \right. \\ &\quad \left. \left. \cdot e^{j2\pi\alpha(m-k)\theta/N} \right) * Q(\alpha) \right\} \right] \\ \frac{d^2\text{Re}\{\gamma(\alpha, \theta)\}}{d\theta^2} &= \frac{1}{K-1} \\ &\quad \cdot \sum_{m=1, m \neq k}^K \left[ \text{Re}\left\{ \left[ X_k(\alpha) \left( \frac{2\pi\alpha(m-k)}{N} \right)^2 \right. \right. \right. \\ &\quad \left. \left. \cdot e^{j2\pi\alpha(m-k)\theta/N} \right] * Q(\alpha) \right\} \right] \\ \text{Im}\{\gamma(\alpha, \theta)\} &= \frac{1}{K-1} \\ &\quad \cdot \sum_{m=1, m \neq k}^K \left[ \text{Im}\{X_k(\alpha) * Q(\alpha)\} \right. \\ &\quad \left. - \text{Re}\left\{ \left( X_k(\alpha) e^{j2\pi\alpha(m-k)\theta/N} \right) * Q(\alpha) \right\} \right] \\ \frac{d\text{Re}\{\gamma(\alpha, \theta)\}}{d\theta} &= \frac{1}{K-1} \\ &\quad \cdot \sum_{m=1, m \neq k}^K \left[ \text{Re}\left\{ \left( X_k(\alpha) \frac{2\pi\alpha(m-k)}{N} \right) \right. \right. \\ &\quad \left. \left. \cdot e^{j2\pi\alpha(m-k)\theta/N} \right) * Q(\alpha) \right\} \right] \\ \frac{d^2\text{Re}\{\gamma(\alpha, \theta)\}}{d\theta^2} &= -\frac{1}{K-1} \\ &\quad \cdot \sum_{m=1, m \neq k}^K \left[ \text{Im}\left\{ \left[ X_k(\alpha) \left( \frac{2\pi\alpha(m-k)}{N} \right)^2 \right. \right. \right. \\ &\quad \left. \left. \cdot e^{j2\pi\alpha(m-k)\theta/N} \right] * Q(\alpha) \right\} \right]. \quad (8) \end{aligned}$$

The mean square error function derived from the maximum likelihood criterion is given by the summation of the errors  $\hat{e}_k^2$ , with  $k = 1, \dots, K$ . Its derivatives are

$$\frac{d\hat{e}_{MLE}^2}{d\theta} = \left(1 - \frac{1}{K}\right) \sum_{k=1}^K \frac{d\hat{e}_k^2}{d\theta} \quad (9)$$

$$\frac{d^2\hat{e}_{MLE}^2}{d\theta^2} = \left(1 - \frac{1}{K}\right) \sum_{k=1}^K \frac{d^2\hat{e}_k^2}{d\theta^2} \quad (10)$$

in which the terms can be computed using (7) and (8). Finally, the following iteration (Newton formula) can be used to find the minimum point of the mse function

$$\hat{\theta}_{i+1} = \hat{\theta}_i - \frac{\frac{d\hat{e}_{MLE}^2(\theta)}{d\theta} \Big|_{\hat{\theta}_i}}{\frac{d^2\hat{e}_{MLE}^2(\theta)}{d\theta^2} \Big|_{\hat{\theta}_i}} \quad i = 0, 1, \dots \quad (11)$$

starting from a coarse estimate  $\hat{\theta}_0$  [36].

The method presented is the extension of that proposed in [19] with the inclusion of a windowing in time domain on the aligned signals with calculation of the optimal delay in the frequency domain. In the following, we will choose for  $p(n)$  a Gaussian window centered at particular instants of time defined on the basis of the burst duration.

#### D. Experimental Protocol

**Subjects:** Ten healthy male subjects [age (mean  $\pm$  SD):  $27.4 \pm 2.4$  years, height:  $177.5 \pm 5.5$  cm, weight:  $72.1 \pm 8.2$  kg] took part in this study. None of the subjects reported symptoms of neuromuscular disorders or problems with the ligaments. The study was approved by the Local Ethics Committee of the Health Department of Region Piemonte and written informed consent was obtained from all participants prior to inclusion.

**Surface EMG Recordings:** Surface EMG signals were detected in single differential configuration during cyclic contractions from the right thigh with two linear adhesive arrays consisting of eight electrodes with 5-mm inter-electrode distance. Vastus lateralis and medialis were the muscles under study. The EMG signals were amplified by a multichannel surface EMG amplifier (EMG 16, LISiN—Prima Biomedical & Sport, Treviso, Italy), bandpass filtered ( $-3$  dB bandwidth = 10–500 Hz), sampled at 2048 samples/s, and converted to digital data by a 12 bit A/D converter board. Before electrode placement, the two muscles were assessed in a few test contractions with a dry array of 16 electrodes (silver bars, 5-mm long, 1-mm diameter, 5-mm inter-electrode distance, Ottino Bioelettronica, Torino, Italy) [40]–[42] with the subject in supine position on a bed. The array was moved over the muscles and the location of the innervation zone was identified by visual analysis of the multi-channel signals [41]. In particular, the innervation zone corresponded to the point of inversion of propagation of the surface detected MUAPs. Two joint angles were considered in this preliminary phase, corresponding to  $75^\circ$  and  $165^\circ$  of leg extension (where  $180^\circ$  represents full extension). The innervation zone location as well as the distal tendon regions were marked over the skin at the two joint angles. The adhesive arrays were located be-

tween the most distal detected innervation zone location and the distal tendon region. The orientation of the array was selected on the basis of visual signal analysis, choosing the angle of inclination which led to most similar potentials traveling along the array. The part of the skin where the location of the arrays was identified was shaved, when necessary, and slightly abraded with abrasive paste (Meditec-Every, Parma, Italy). A reference electrode was placed at the right wrist.

**General Procedures:** After placement of the two electrode arrays, the subject was asked to sit on a cycle-ergometer (model Powerbike, Panatta Sport, Macerata, Italy), on which an angular velocity sensor was mounted. An electronic goniometer was fixed on the subject's right leg (Fig. 1). The subject was then asked to cycle at a constant average velocity of 60 cycles/min. The average power exerted was 150 W. The signal recording started a few seconds before the cycling task to provide reference noise levels at the beginning of the contraction. A visual display of average cycling velocity was provided to the subject. The task lasted 4 min. After the cycling task, the subcutaneous layer thickness was measured with an ecograph (Fukuda Denshi, model FF SONIC UF-4000L) for both muscles. Anatomical measures were taken to document electrode positioning and innervation zone location.

**Data Processing:** The intervals of activity of the two muscles were identified from the EMG signals as described above [32]. The algorithm for detection of muscle activity was applied to the single differential recordings. An interval of 200 ms at the beginning of the recording was considered as containing only noise and used for the determination of the threshold for activation interval detection. The first five activation intervals were excluded from further analysis since they represented the starting phase of the cycling task.

The time duration of each detected EMG burst was normalized to 100% and three locations within the bursts were analyzed, corresponding to 25%, 50%, and 75% of the burst duration. Double differential signals were computed by subtraction of adjacent single differential signals and considered for further analysis [43]. CV was estimated from double differential signals at the three selected locations with Gaussian windows (4) of standard deviation 25, 50, and 100 ms. CV was estimated with the proposed iterative technique in the frequency domain from two to six channels for each muscle, burst, window width, and location within the burst. The maximum of the cross-correlation function between signal pairs was used to assess signal similarity and, thus, the quality of the CV estimate.

**Statistical Analysis:** The CV values over time were fitted with second order polynomial functions and the root mse in the different conditions was evaluated with respect to this polynomial fitting. Initial values and slopes of CV were defined as the intercept and first derivative at time zero of the second order polynomial function interpolating the data. Normalized slopes were computed as the slopes divided by the initial values. Results were analyzed using one-, two-, and three-way repeated measures analysis of variance (ANOVA), followed by *post-hoc* Student-Newman-Keuls (SNK) pair-wise comparisons, when required. Student t-test was also used for some comparisons. Statistical significance was set to  $\alpha = 0.05$ . Data are reported as mean  $\pm$  SD in the text and mean  $\pm$  standard error of the mean (SE) in the figures.

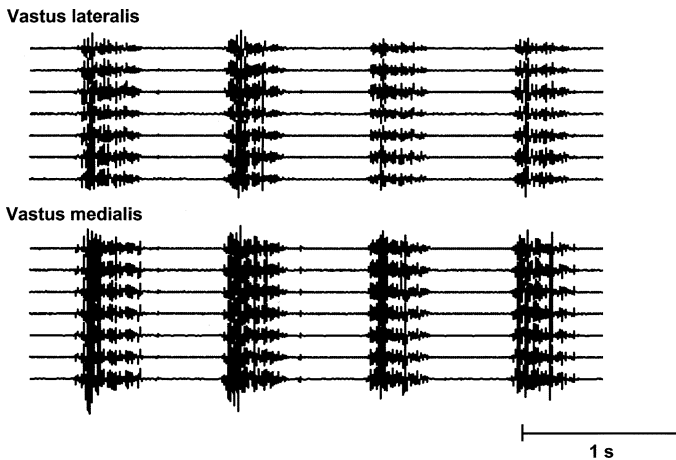


Fig. 3. Surface EMG signals detected from the vastus lateralis and vastus medialis muscles during a cycling exercise. The seven single differential signals detected by each array are shown. Normalized amplitude units are used.

### III. RESULTS

Representative signals detected during the cycling task are reported in Fig. 3. Note the absence of significant movement artifacts for all the detected channels.

#### A. Subcutaneous Fat Layer Thickness, Innervation Zone Location, and Electrode Placement

The thickness of the subcutaneous fat layer was (mean  $\pm$  SD, across subjects)  $4.2 \pm 1.5$  mm and  $3.3 \pm 0.9$  mm for vastus lateralis and vastus medialis, respectively. The innervation zone location at  $165^\circ$  joint angle was at a distance from the apex patella of  $10.3 \pm 2.5$  cm, for vastus lateralis, and  $5.9 \pm 2.4$  cm, for vastus medialis. At  $75^\circ$ , the innervation zone was located at  $9.5 \pm 2.6$  cm and  $5.6 \pm 2.3$  cm distance from the apex patella for vastus lateralis and vastus medialis, respectively. The angle of inclination of the array with respect to the line between the most prominent point of the iliac crest and the apex patella was  $27.5 \pm 7.3^\circ$  (laterally) for vastus lateralis, and  $55.8 \pm 13.5^\circ$  (medially) for vastus medialis (Fig. 1).

#### B. Intervals of Muscle Activity

Fig. 4 shows an example of determination of intervals of muscle activity for a single channel. A detail of a detected burst is also shown. Table I summarizes the data regarding activation interval duration and speed during muscle activity. There was no statistical difference between the two muscles in average (over all bursts) activation interval duration, starting and ending joint angles of activation, angles at which the windows were located, and angular velocity at the window locations (paired Student *t*-tests). For both muscles, average (over all bursts) angular velocity statistically increased with window location (one-way ANOVA with factor the window location and *post-hoc* SNK test,  $p < 0.001$ ).

#### C. CV Estimate Standard Deviation, Initial Values, and Slopes: Effect of Number of Channels and Window Duration

Fig. 5 shows an example of windows applied at the three locations in a burst of EMG activity. Double differential signals

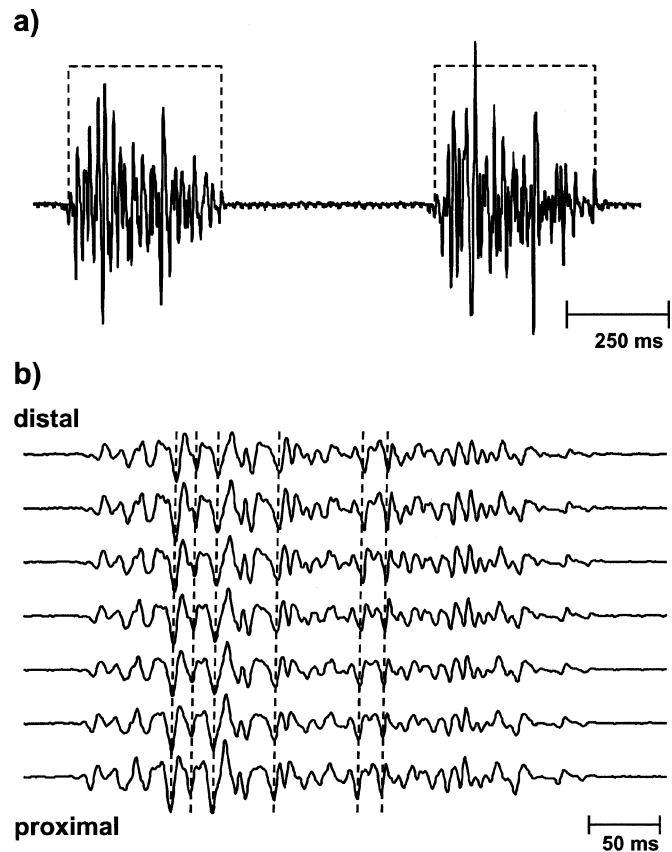


Fig. 4. (a) Example of application of the algorithm for estimation of muscle activation intervals. The signals are detected from the vastus lateralis muscle. The dashed line indicates the activation intervals as detected by the algorithm. (b) Examples of single differential multichannel surface EMG signals detected from the vastus medialis muscle during a cycling exercise. One burst of activity is shown. The dashed lines indicate the propagation of the action potentials. Note the similarity among the potentials detected at the different channels; also note that, for the entire burst, all the channels present propagating potentials. During the time interval of the burst the joint angle changes by approximately  $40^\circ$  (see Table I).

detected from the different channels are also compared to show their similar shape. The maximum of the cross-correlation function between double differential signals detected on different channels within the bursts (considering all the possible signal pairs) was on average (mean  $\pm$  SD, over all subjects; one value for each subject and muscle representing the average value over all bursts)  $0.82 \pm 0.08$ . This value suggests a reliable estimate of CV.

A two-way (factors: number of channels and Gaussian window width) ANOVA of the root mse of CV estimation with respect to the polynomial fitting was significant for both factors ( $p \ll 0.001$  and  $p < 0.05$ , respectively). CV root mse significantly decreased with increasing number of channels and window width. It was statistically different with two and three channels with respect to all the other cases (SNK test,  $p < 0.001$ ) (Fig. 6). There was a significant difference (SNK test,  $p < 0.05$ ) in CV root mse with the shortest (25-ms standard deviation) and the longest (100 ms) window (Fig. 6). Using the maximum number of channels, CV root mse decreased with window width but very slightly (Fig. 6).

TABLE I  
SUMMARY OF PARAMETERS (MEAN  $\pm$  SD, ACROSS SUBJECTS) RELATIVE TO THE BEGINNING AND END OF BURST OF ACTIVATION, AND TO THE POSITION OF THE WINDOW FOR CV ESTIMATION IN VASTUS LATERALIS AND MEDIALIS MUSCLE DURING THE CYCLING TASK ANALYZED

		Vastus lateralis	Vastus medialis
Joint angle at start of bursts		$(78.9 \pm 6.5)^\circ$	$(79.5 \pm 7.0)^\circ$
Joint angle at end of bursts		$(121.3 \pm 6.5)^\circ$	$(121.6 \pm 5.4)^\circ$
Burst duration		$(42.4 \pm 6.9)^\circ$ $(385.3 \pm 47.1)$ ms	$(42.1 \pm 6.4)^\circ$ $(398.5 \pm 55.1)$ ms
Joint angle at specified percentages of burst duration	25%	$(78.5 \pm 6.8)^\circ$	$(78.2 \pm 6.9)^\circ$
	50%	$(87.9 \pm 4.9)^\circ$	$(87.3 \pm 4.8)^\circ$
	75%	$(104.1 \pm 4.6)^\circ$	$(103.8 \pm 3.6)^\circ$
Instantaneous speed at specified percentages of burst duration	25%	$(51.1 \pm 15.0)^\circ/\text{s}$	$(43.7 \pm 20.6)^\circ/\text{s}$
	50%	$(138.8 \pm 37.9)^\circ/\text{s}$	$(135.3 \pm 39.5)^\circ/\text{s}$
	75%	$(187.4 \pm 31.1)^\circ/\text{s}$	$(188.6 \pm 33.3)^\circ/\text{s}$

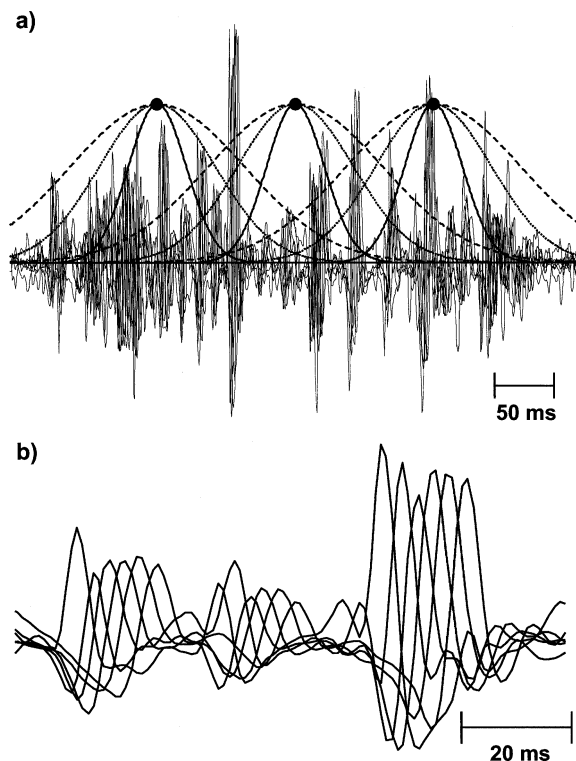


Fig. 5. (a) A burst of signal activity detected from the vastus lateralis muscle. The six double differential signals are superimposed. The windows applied to the mse function are represented in the three locations and for the three standard deviations (25 ms—solid lines, 50 ms—dotted lines, 100 ms—dashed lines). (b) A detail of the burst shown in a) with the six double differential signals superimposed. Note the stability of the recording and the similarity in shape of the signals detected at the different channels.

A one-way ANOVA (factor: number of channels) of CV initial values, slopes, and normalized slopes was not significant. Results obtained with the maximum number of channels available, leading to the lowest root mse of CV estimation, will be reported in the following.

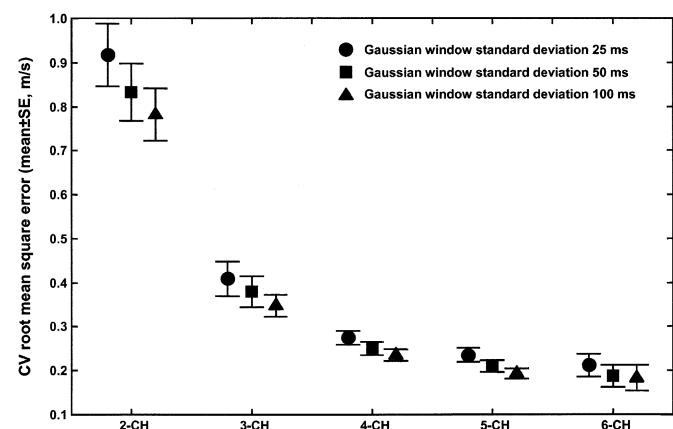


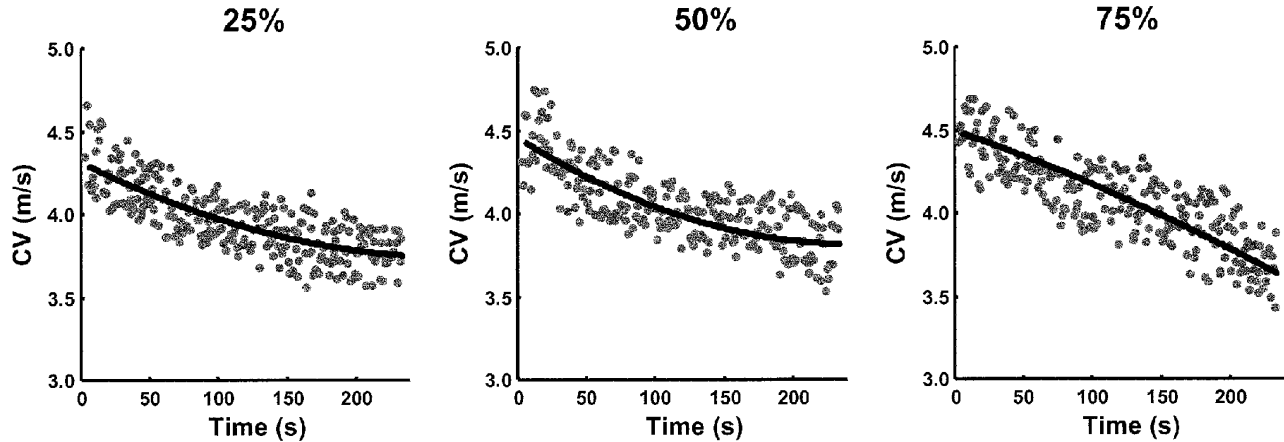
Fig. 6. Root mse (mean  $\pm$  SE, across subjects and muscles) of CV estimates as a function of the number of double differential signals used for the estimation and for the three window widths.

#### D. CV Initial Values and Slopes

A typical pattern of CV for the two muscles is shown in Fig. 7. A three-way ANOVA (factors: window width, muscle, location of the window) of CV initial values was not significant for any of the factors. There was, however, a tendency of CV initial values to increase from the first to the last location [Fig. 8(a)].

CV slopes and normalized slopes were statistically different from zero and negative for both muscles (Student t-test including all subjects). A three-way ANOVA (factors: window width, muscle, location of the window) of CV slope was significant for the muscle ( $p < 0.01$ ) and for the location of the window ( $p < 0.05$ ). Vastus medialis resulted in higher slopes (absolute values) than vastus lateralis muscle (SNK test,  $p < 0.01$ ) and there was a significant tendency of the slope to increase (absolute values) from the first to the last window location, with the first location statistically different from the third (SNK test,  $p < 0.05$ ) [Fig. 8(b)]. Normalized CV slopes led to similar results as the slopes.

### Vastus lateralis



### Vastus medialis

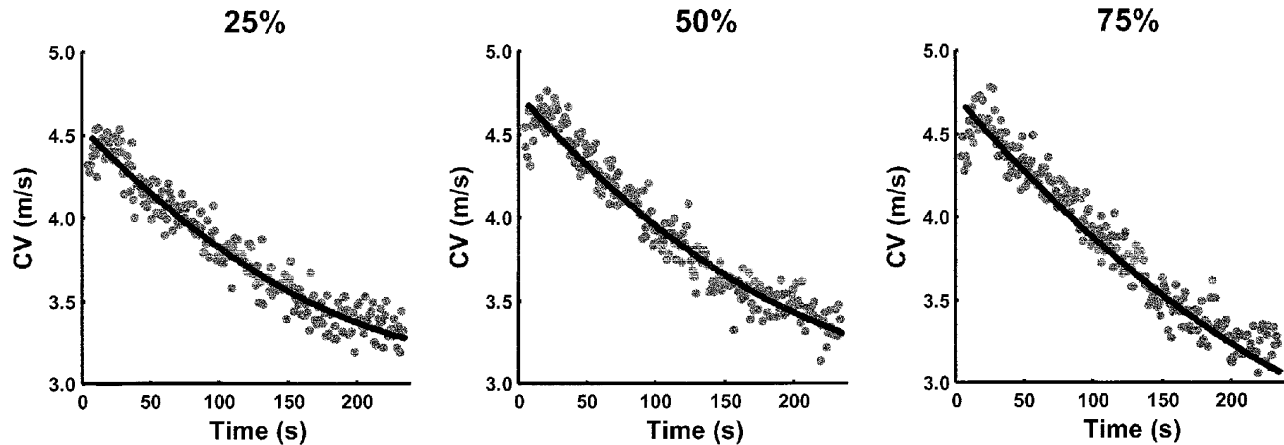


Fig. 7. CV estimates during the 4-min contraction for the vastus lateralis and medialis muscles of one subject, computed from six double differential signals in the three locations within the bursts (25-ms window standard deviation). The second-order polynomial function interpolating the estimates is shown in bold black line.

#### E. Correlation Among CV Estimates

The correlation coefficient between CV estimates in the three locations (average over all the location pairs), using the maximum number of channels, was (mean  $\pm$  SD, across subjects)  $0.60 \pm 0.15$ ,  $0.77 \pm 0.11$ , and  $0.93 \pm 0.07$ , for the 25-, 50-, and 100-ms window standard deviation, respectively.

#### IV. DISCUSSION

In this study, we proposed a set of procedures and signal processing techniques to assess global muscle CV from surface EMG signals detected during dynamic contractions involving fast limb movements. Estimating directly muscle fiber CV has advantages with respect to spectral analysis since CV is a direct physiological parameter. In dynamic contractions, with recruitment/de-recruitment of MUs, modulation of MU firing rate, and short muscle activation intervals, the interpretation of spectral features is subject to many theoretical and practical problems. Reliable assessment of CV is preferable, although important technical problems in both signal detection and processing arise.

Arrays of sensors with fixed inter-electrode distance, not sensitive to movement artifacts, are needed for signal detection

during movement. Arrays made of metal electrodes are critical in this respect. The adhesive linear electrode arrays used in this study are suitable for detecting traveling signals along the muscle fibers with negligible movement artifacts (Figs. 2, 4, and 5). The experimental signals detected at the different channels during the bursts of activity had indeed very similar shapes, as assessed by a correlation coefficient higher than 0.8, on average.

From the signal processing point of view, two main issues should be addressed: 1) the standard deviation of the estimates obtained during movement should be low enough to detect small differences between different muscle conditions and 2) short signal portions should be analyzed since there may be changes in the type of MUs activated in a short interval of time. From past work [3], [19], it was evident that two-channel based methods for CV assessment result in large standard deviation of estimation. In the dynamic condition analyzed, the root mse of CV estimates was of the order of 0.8 m/s using two EMG channels (Fig. 6). With the multichannel method proposed, the root mse of CV estimates could be reduced to approximately 0.2 m/s (Fig. 6). This value is only slightly higher than that obtained by multichannel methods in the case of isometric, constant force contractions or of CV estimation from single



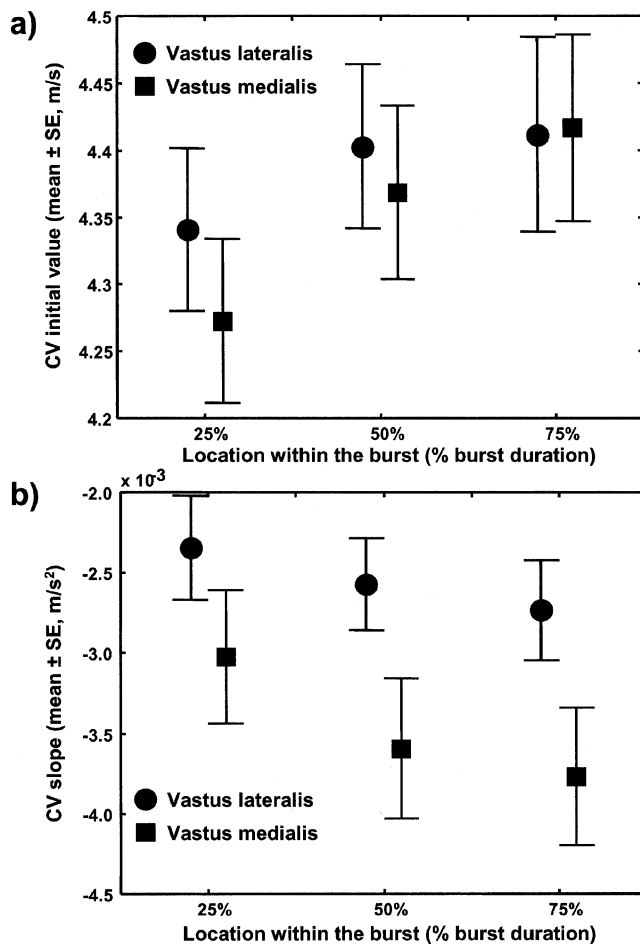


Fig. 8. (a) CV initial values and (b) slopes (mean  $\pm$  SE; averages over all the window widths and for the estimates from the maximum number of channels) for the two muscles and the three locations within the bursts.

MUs, using the same spatial filter applied in this study [3], [19]. Isometric contractions lead to quasistationary signals in much more standardized conditions with respect to those of the present study, thus the slight difference in the root mse of CV estimates with respect to the dynamic case is somehow surprising.

The variability of the CV estimates depended only to a minor extent on the window duration adopted. Short windows, giving detailed indication on the type of MUs activated in a particular time interval within the burst, can thus be applied. The small increase of CV root mse with decreasing window width is due to the decreasing number of available samples for delay estimation. Moreover, decreasing the window width, the number of action potentials contributing to the CV estimate decreases. Since the MUs have a distribution of CVs, smaller window widths may lead to a smaller sample of MUAPs and thus to a larger variability of the estimate. On the other hand, the method proposed avoids any signal truncation, thus reduction in window width is not critical from this point of view.

The CV estimates obtained in this study were within physiological values and a significant decrease with time was observed during the cycling task for both muscles (e.g., Fig. 7), reflecting myoelectric manifestations of muscle fatigue. In the cycling task

investigated, the rate of change of CV was larger for vastus medialis than for vastus lateralis (Figs. 7 and 8) which may indicate a different degree of activation of the two muscles during the task, i.e., different force levels exerted. The result may also reflect a different proportion of type II fibers detected from the vastus medialis.

There was a significant tendency for higher CV decrease with increasing the instantaneous velocity of cycling (Fig. 7; note that the instantaneous velocity increases with the window location within the burst, as reported in Table I). This may reflect different MUs recruited depending on the velocity of the movement or a different average firing rate of the recruited MUs since single MU CV changes with changes in firing rate. The large significant difference which was detected between CV slopes estimated from the three locations within the same bursts (Fig. 8) is interesting considering that the locations were separated by only about 100 ms between each other. In this time interval, the signal is highly nonstationary. The technique allows to reliably detect changes in muscle activity even from very short bursts typical of dynamic conditions.

The present techniques can be applied in a number of conditions, including gait analysis and sport performance. However, the limitations of the approach should be properly outlined for its best application. First, the muscles from which CV can be reliably estimated are in limited number. They should have long and parallel fibers with innervation zones concentrated in a small muscle region. During movement, the innervation zone shift and muscle shortening limit the portion of fiber semi-length from which propagating signals can be detected at all the joint angles of interest. If the range of movement is limited, the latter may be a minor problem but, in general, it may limit the applicability of the method. Different muscles present different degrees of movement with respect to the skin with changes of joint angle; the muscles selected in this study showed a shift of the innervation zone limited to 10–15 mm over the full range of movement, as found in a previous work [31], and were suited for CV estimation in a large range of joint angles (see also Fig. 4). If the shift is larger, the best channels should be selected in each condition on the basis of shape similarity between signals or more sophisticated criteria.

Placement of the electrodes is critical for CV estimation and expert operators are required for this operation. Indeed, the anatomical muscle fiber properties should be assessed by analysis of the detected signals and the optimal array orientation should be selected. Apart from the inherent difficulties in applying the technique, there are also many methodological issues not yet addressed and which should be investigated in future studies. CV estimates depend on the relative weight of end-plate and end-of-fiber components in the signal, which are nontraveling. The relative weight of nontravelling signals depends on the thickness of subcutaneous layers [9], distance of the detection system from the innervation zone and tendon [44], and crosstalk from nearby muscles [45]. In some muscles these factors may be dominant, thus prevalence of nontravelling signals is often observed (e.g., [46]). Moreover, the relative importance of these factors may change during a dynamic contraction at the different joint angles. The suggested way of placing electrodes may limit the bias of CV estimates during

movement but it is not clear how practically these effects influence the estimates. If relative changes of CV are analyzed at the same joint angles (as in the present study for each window location), these problems may have minor relevance. Difficulties arise when comparing estimates obtained at different joint angles or from different muscles. For example, the small increase of CV with joint angle (i.e., with window location within the burst; Fig. 8) may be interpreted as reflecting different MU recruitment or due to different proportion of nontravelling signals in the two conditions. The same applies when comparing initial CV values from vastus lateralis and medialis. In addition to nontravelling components, different relative orientations of the fibers with respect to the line of the electrodes may play a role in comparing the results and relative orientation of the fibers may change at different joint angles.

The cycling task allows for the assessment of CV changes by analyzing signals detected at the same joint angle during time. This condition excludes many of the methodological issues discussed above. Relative changes of CV observed during time at fixed locations within the bursts [Fig. 8(b)] can thus be considered as reflecting different changes in the properties of the MUs analyzed at the different burst locations.

## V. CONCLUSION

The main conclusions of this study are: 1) traveling signals along the muscle fibers were recorded with negligible movement artifacts in dynamic conditions involving fast movements; 2) CV was thus estimated in these conditions; 3) multichannel CV estimates had a root mse of the order of 0.2 m/s; 4) the width of the window used for CV estimation only slightly affected CV estimation standard deviation; 5) a trend of decreasing CV, reflecting fatigue, could be observed in the specific dynamic task analyzed; 6) the two muscles analyzed showed significantly different rate of change of CV during the task; and 7) it was possible to statistically distinguish the decrease of CV as estimated at different instantaneous angular velocities within the same bursts of signal activity.

Within the limitations discussed, the techniques presented in this work represent powerful new tools for noninvasive muscle assessment and open interesting perspectives in motor control studies during dynamic conditions. In particular, they provide the means for interpreting myoelectric manifestations of muscle fatigue in dynamic contractions in a less speculative way than has been previously possible.

## REFERENCES

- [1] S. Andreassen and L. Arendt-Nielsen, "Muscle fiber conduction velocity in motor units of the human anterior tibial muscle: A new size principle parameter," *J. Physiol.*, vol. 391, pp. 561–71, 1987.
- [2] L. Arendt-Nielsen and M. Zwarts, "Measurement of muscle fiber conduction velocity in humans: Techniques and applications," *J. Clin. Neurophysiol.*, vol. 6, pp. 173–90, 1989.
- [3] D. Farina, L. Arendt-Nielsen, R. Merletti, and T. Graven-Nielsen, "Assessment of single motor unit conduction velocity during sustained contractions of the tibialis anterior muscle with advanced spike triggered averaging," *J. Neurosci. Methods*, vol. 115, pp. 1–12, 2002.
- [4] R. Merletti and C. J. De Luca, "New techniques in surface electromyography," in *Computer Aided Electromyography and Expert Systems*, J. E. Desmedt, Ed. New York: Elsevier, 1989.
- [5] H. J. Huppertz, C. Disselhorst-Klug, J. Silny, G. Rau, and G. Heimann, "Diagnostic yield of noninvasive high-spatial-resolution-EMG in neuromuscular disease," *Muscle & Nerve*, vol. 20, pp. 1360–1370, 1997.
- [6] T. Sadoyama, T. Masuda, H. Miyata, and S. Katsuta, "Fiber conduction velocity and fiber composition in human vastus lateralis," *Eur. J. Appl. Physiol.*, vol. 57, pp. 767–771, 1988.
- [7] W. Troni, R. Cantello, and I. Rainero, "Conduction velocity along human muscle fibers in situ," *Neurology*, vol. 33, pp. 1453–1459, 1983.
- [8] M. J. Zwarts, "Evaluation of the estimation of muscle fiber conduction velocity. Surface versus needle method," *J. Neurophysiol.*, vol. 83, pp. 441–452, 1989.
- [9] D. Farina, C. Cescon, and R. Merletti, "Influence of anatomical, physical and detection system parameters on surface EMG," *Biol. Cybern.*, vol. 86, pp. 445–456, 2002.
- [10] L. Lindstrom and R. Magnusson, "Interpretation of myoelectric power spectra: A model and its applications," *Proc. IEEE*, vol. 65, pp. 653–662, 1977.
- [11] L. Arendt-Nielsen and K. R. Mills, "The relationship between mean power frequency of the EMG spectrum and muscle fiber conduction velocity," *Electroencephalogr. Clin. Neurophysiol.*, vol. 60, pp. 130–134, 1985.
- [12] F. B. Stulen and C. J. DeLuca, "Frequency parameters of the myoelectric signal as a measure of muscle conduction velocity," *IEEE Trans. Biomed. Eng.*, vol. BME-28, pp. 512–522, 1981.
- [13] M. Bernardi, M. Solomonow, G. Nguyen, A. Smith, and R. Baratta, "Motor unit recruitment strategies changes with skill acquisition," *Eur. J. Appl. Physiol.*, vol. 74, pp. 52–59, 1996.
- [14] P. Bonato, S. H. Roy, M. Knaflitz, and C. J. DeLuca, "Time-frequency parameters of the surface myoelectric signal for assessing muscle fatigue during cyclic dynamic contractions," *IEEE Trans. Biomed. Eng.*, vol. 48, pp. 745–753, July 2001.
- [15] S. Karlsson, J. Yu, and M. Akay, "Time-frequency analysis of myoelectric signals during dynamic contractions: A comparative study," *IEEE Trans. Biomed. Eng.*, vol. 47, pp. 228–238, Feb. 2000.
- [16] D. MacIsaac, P. A. Parker, and R. N. Scott, "The short-time fourier transform and muscle fatigue assessment in dynamic contractions," *J. Electromyogr. Kinesiol.*, vol. 11, pp. 439–449, 2001.
- [17] S. H. Roy, P. Bonato, and M. Knaflitz, "EMG assessment of back muscle function during cyclical lifting," *J. Electromyogr. Kinesiol.*, vol. 8, pp. 233–245, 1998.
- [18] D. Farina, E. Fortunato, and R. Merletti, "Non-invasive estimation of motor unit conduction velocity distribution using linear electrode arrays," *IEEE Trans. Biomed. Eng.*, vol. 41, pp. 380–388, Feb. 2000.
- [19] D. Farina, W. Muhammad, E. Fortunato, O. Meste, R. Merletti, and H. Rix, "Estimation of single motor unit conduction velocity from surface electromyogram signals detected with linear electrode arrays," *Med. Biol. Eng. Comput.*, vol. 39, pp. 225–236, 2001.
- [20] D. Farina and R. Merletti, "A novel approach for estimating muscle fiber conduction velocity from spatial and temporal filtering of surface EMG signals," *IEEE Trans. Biomed. Eng.*, vol. 50, pp. 1340–1351, Dec. 2003.
- [21] —, "Comparison of algorithms for estimation of EMG variables during voluntary isometric contractions," *J. Electromyogr. Kinesiol.*, vol. 10, pp. 337–350, 2000.
- [22] D. Farina, M. Fosci, and R. Merletti, "Motor unit recruitment strategies investigated by surface EMG variables," *J. Appl. Physiol.*, vol. 92, pp. 235–247, 2002.
- [23] L. Lindstrom, R. Magnusson, and I. Petersen, "Muscular fatigue and action potential conduction velocity changes studied with frequency analysis of EMG signals," *Electromyography*, vol. 10, pp. 341–56, 1970.
- [24] G. N. McVicar and P. A. Parker, "Spectrum dip estimator of nerve conduction velocity," *IEEE Trans. Biomed. Eng.*, vol. 35, pp. 1069–1076, Dec. 1988.
- [25] E. Schulte, D. Farina, G. Rau, R. Merletti, and C. Disselhorst-Klug, "Analysis of single motor unit properties from spatially filtered surface EMG signals—Part II: Conduction velocity estimation," *Med. Biol. Eng. & Comput.*, vol. 41, pp. 338–45, 2003.
- [26] A. Bottin and P. Rebecchi, "Impedance and noise of the skin-electrode interface in surface EMG recordings," in *Proc. XIVth ISEK Congr.*, Vienna, Austria, 2002, pp. 246–247.
- [27] M. Pozzo, D. Farina, and R. Merletti, "Electromyography: Detection, processing and applications," in *Handbook of Biomedical Technology and Devices*, J. E. Moore, Ed. Boca Raton, FL: CRC Press, 2003, ch. 4.
- [28] W. Li and K. Sakamoto, "The influence of location of electrode on muscle fiber conduction velocity and EMG power spectrum during voluntary isometric contractions measured with surface array electrodes," *Appl. Human Sci.*, vol. 15, pp. 25–32, 1996.

- [29] S. H. Roy, C. J. De Luca, and J. Schneider, "Effects of electrode location on myoelectric conduction velocity and median frequency estimates," *J. Appl. Physiol.*, vol. 61, pp. 1510–1517, 1986.
- [30] D. MacIsaac, P. A. Parker, and K. Englehart, "Feasibility of conduction velocity as a fatigue index in dynamic contractions," in *Proc. XIVth ISEK Congress*, Vienna, Austria, 2002, pp. 179–180.
- [31] D. Farina, R. Merletti, M. Nazzaro, and I. Caruso, "Effect of joint angle on surface EMG variables for the muscles of the leg and thigh," *IEEE Eng. Med. Biol. Mag.*, vol. 20, pp. 62–71, 2001.
- [32] A. Merlo, D. Farina, and R. Merletti, "A fast and reliable technique for muscle activity detection from surface EMG signals," *IEEE Trans. Biomed. Eng.*, vol. 50, pp. 316–323, Mar. 2003.
- [33] S. Davies and P. Parker, "Estimation of myoelectric conduction velocity distribution," *IEEE Trans. Biomed. Eng.*, vol. BME-34, pp. 98–105, 1987.
- [34] I. W. Hunter, R. E. Kearney, and L. A. Jones, "Estimation of the conduction velocity of muscle action potentials using phase and impulse response function techniques," *Med. Biol. Eng. Comp.*, vol. 25, pp. 121–126, 1987.
- [35] L. Lo Conte and R. Merletti, "Advances in processing of surface myoelectric signals: Part 2," *Med. Biol. Eng. Comput.*, vol. 33, pp. 362–372, 1995.
- [36] K. C. McGill and L. J. Dorfman, "High resolution alignment of sampled waveforms," *IEEE Trans. Biomed. Eng.*, vol. BME-31, pp. 462–470, 1984.
- [37] R. Merletti and L. Lo Conte, "Advances in processing of surface myoelectric signals: Part 1," *Med. Biol. Eng. Comput.*, vol. 33, pp. 373–384, 1995.
- [38] O. Meste, W. Muhammad, H. Rix, and D. Farina, "On the estimation of muscle fiber conduction velocity using a co-linear electrode array," in *Proc. 23rd Annu. Int. Conf. IEEE Engineering in Medicine and Biology Society*, Istanbul, Turkey, 2001.
- [39] J. Schneider, G. Rau, and J. Silny, "A noninvasive EMG technique for investigating the excitation propagation in single motor units," *Electromyogr. Clin. Neurophysiol.*, vol. 29, pp. 273–280, 1989.
- [40] R. Merletti, D. Farina, and M. Gazzoni, "The linear electrode array: A useful tool with many applications," *J. Electromyogr. Kinesiol.*, vol. 13, pp. 37–47, 2003.
- [41] T. Masuda, H. Miyano, and T. Sadoyama, "The position of innervation zones in the biceps brachii investigated by surface electromyography," *IEEE Trans. Biomed. Eng.*, vol. BME-32, pp. 36–42, Jan. 1985.
- [42] R. Merletti, D. Farina, and A. Granata, "Non-invasive assessment of motor unit properties with linear electrode arrays," in *Clinical Neurophysiology: From Receptors to Perception*. New York: Elsevier, 1999, ch. 34, pp. 293–300.
- [43] H. Broman, G. Bilotto, and C. J. De Luca, "A note on noninvasive estimation of muscle fiber conduction velocity," *IEEE Trans. Biomed. Eng.*, vol. BME-32, pp. 311–319, 1985.
- [44] A. Gydikov, L. Gerilovski, N. Radicheva, and N. Troyanova, "Influence of the muscle fiber end geometry on the extracellular potentials," *Biol. Cybern.*, vol. 54, pp. 1–8, 1986.
- [45] D. Farina, R. Merletti, B. Indino, M. Nazzaro, and M. Pozzo, "Cross-talk between knee extensor muscles. Experimental and modeling results," *Muscle Nerve*, vol. 26, pp. 681–95, 2002.
- [46] D. Farina, M. Gazzoni, and R. Merletti, "Assessment of low back muscle fatigue by surface EMG signal analysis: Methodological aspects," *J. Electromyogr. Kinesiol.*, vol. 13, pp. 319–332, 2003.



**Dario Farina** (M'01) graduated in electronics engineering (*summa cum laude*) from the Politecnico di Torino, Torino, Italy, in 1998 and received the Ph.D. degree in electronics engineering from the Politecnico di Torino and the Ecole Centrale de Nantes, Nantes, France, in 2001.

During 1998, he was a Fellow of the Laboratory for Neuromuscular System Engineering, Torino. Since 1999, he has been involved in teaching activities in electronics and mathematics at the Politecnico di Torino, and since 2002, he has been a Research

Assistant Professor at the Politecnico di Torino. He acts as referee for many scientific international journals and is on the Editorial Board of the *Journal of Electromyography and Kinesiology*. His main research interests are in the areas of signal processing applied to biomedical signals, modeling of biological systems, and basic and applied physiology of the neuromuscular system.

Dr. Farina is a Registered Professional Engineer.



**Marco Pozzo** graduated in electronics engineering from the Politecnico di Torino, Torino, Italy, in October 1998.

He was an External Consultant for the Laboratory for Neuromuscular System Engineering (LISiN), Torino, during 1998, and since 1999, has been a Design Manager in the LISiN Hardware Laboratory. Since 2001, he has also been an Assistant Coordinator of the European RTD Project "Neuromuscular assessment in the Elderly Worker" and has been involved in three research projects in collaboration

with the European Space Agency. He is co-author of a chapter in the Handbook of Biomedical Technology and Devices (Boca Raton, FL: CRC Press, 2003). His main research activities concern the design of biomedical devices and their application to the assessment of the neuromuscular system.



**Enrico Merlo** graduated in electronics engineering from the Politecnico di Torino, Torino, Italy, in July 2001, with a thesis on bioengineering.

Since July 2001 he is a Fellow of the Laboratory for Neuromuscular System Engineering (LISiN) in Torino, Italy. At LISiN, he is currently involved in projects for the evaluation of methods for the assessment of muscle conditions in dynamic exercises, with applications in both basic and applied physiology. His main research interests are in the design of biomedical instrumentation, especially for the detection of myoelectric signals and the measurement of biomechanical variables, signal processing, and physiology of the neuromuscular system.

Mr. Merlo is a Registered Professional Engineer.



**Andrea Bottin** was born in Chivasso, Italy, in 1973. He graduated in electronics engineering from the Politecnico di Torino, Torino, Italy, in 1999.

Since 1999, his research activities have been in the field of electromyography at the Laboratory for Neuromuscular System Engineering (LISiN), Torino, specifically in the design and engineering of innovative EMG sensors. Since 2001, he has also been involved in the technological transfer toward companies. He is active in applied research European projects.



**Roberto Merletti** (S'71–M'72) graduated in electronics engineering from the Politecnico di Torino, Italy, and received the M.S. and Ph.D. degrees in biomedical engineering from The Ohio State University.

Since 1984, he has been an Associate Professor of Biomedical Instrumentation with the Department of Electronics, Politecnico di Torino. From 1989 to 1994, he was an Associate Professor at the Department of Biomedical Engineering, Boston University, Boston, MA, and a Research Associate at the Neuromuscular Research Center of the same university. In 1996, he founded the Laboratory for Neuromuscular System Engineering at Politecnico di Torino, where he is currently Director. He is the Coordinator of a project sponsored by the European Community and of a project sponsored by the European Space Agency. His research focuses on detection, processing, and interpretation of surface EMG and on electrical stimulation and neuromuscular control.